Ruthenium(II)-Catalyzed Hydrogenation of Carbon Dioxide to Formic Acid. Theoretical Study of Significant Acceleration by Water Molecules

Yu-ya Ohnishi,[†] Yoshihide Nakao,[†] Hirofumi Sato,[†] and Shigeyoshi Sakaki*[,†,‡]

Department of Molecular Engineering, Graduate School of Engineering, Kyoto University, Nishikyo-ku, Kyoto 615-8510, Japan, and Fukui Institute for Fundamental Chemistry, Kyoto University, Nishihiraki-cho, Takano, Sakyo-ku, Kyoto 606-8103, Japan

Received April 5, 2006

Ru-catalyzed hydrogenation of carbon dioxide to formic acid was theoretically investigated with DFT and MP4(SDQ) methods. In the presence of water molecules, the reaction proceeds as follows: (1) Carbon dioxide forms the adduct *cis*-$Ru(H)_2(PMe_3)_3(H_2O)(CO_2)$, in which the C and O atoms of CO_2 interact with the H (hydride) ligand and the H atom of H_2O, respectively. (2) Nucleophilic attack of the H ligand to CO_2 takes place easily to afford a Ru-(η^1-formate) intermediate, $Ru(H)(PMe_3)_3(\eta^1\text{-}OCOH)(H_2O)$, with a much smaller activation barrier than that of the CO_2 insertion into the Ru−H bond, which is the rate-determining step in the absence of water molecules. (3) The rate-determining step is the coordination of a dihydrogen molecule with the Ru-(η^2-formate) complex, $Ru(H)(PMe_3)_3(\eta^2\text{-}O_2CH)(H_2O)$, the activation barrier of which is smaller than that of the CO_2 insertion into the Ru−H bond. (4) The metathesis of the Ru-(η^1-fomate) moiety with the dihydrogen molecule easily occurs in $Ru(H)(PMe_3)_3(\eta^1\text{-}OCOH)(H_2)(H_2O)$ to afford formic acid with a moderate activation barrier. On the basis of these results, it should be concluded that the early half of the reaction mechanism changes by the presence of water molecules, which is the reason for the acceleration by water molecules. One of the most important results is that the aqua ligand accelerates the nucleophilic attack of the H ligand to CO_2 because the hydrogen-bonding interaction between the aqua ligand and carbon dioxide decreases the activation barrier and increases the exothermicity. Theoretical calculations clearly show that similar acceleration is induced by amines and alcohols.

Introduction

Catalytic hydrogenation of carbon dioxide by transition-metal complexes is one of the most important and the most interesting subjects of research in recent transition-metal chemistry, catalytic chemistry, and organometallic chemistry.[1] The first report was presented by Inoue and his collaborators in 1976.[2] They successfully carried out this hydrogenation reaction with M(diphos) (M = Ni or Pd), $Pd(PPh_3)_4$, $RhCl(PPh_3)_3$, $RuH_2(PPh_3)_4$, and $IrH_3(PPh_3)_3$ in the presence of amine. However, the turnover numbers reported were small. Since this first report, a lot of studies have been carried out on the hydrogenation of carbon dioxide. For instance, Darensbourg and his collaborators performed the hydrogenation of carbon dioxide with $[MH(CO)_6]^-$ (M = Cr, Mo, or W) in 1984.[3] In 1989, Taqui Kahn and his collaborators applied $[Ru(edtaH)Cl]^-$ to the hydrogenation and reported somewhat large turnover numbers of about 180.[4] In 1992, Tsai and his collaborator[5] and Leitner and his collaborators[6] successfully carried out Rh(III)- and Rh(I)-catalyzed hydrogenation of carbon dioxide, respectively. In 1994, Jessop, Ikariya, and Noyori performed an extremely efficient hydrogenation of carbon dioxide with $RuX(Y)(PMe_3)_4$ (X, Y = H, Cl, or O_2CMe).[7] This report draws a lot of attention because of the extremely high turnover numbers. The other interesting result reported is that a small amount of water significantly enhances the catalytic efficiency. Later, a similar promotion effect of water in the Ru-catalyzed hydrogenation was reported by a different group, where a ruthenium complex, $TpRuH(PPh_3)(CH_3CN)$ (Tp = hydrotris(pyrazolyl)borate), was employed as a catalyst.[8] Also, not only water but also various alcohols accelerate hydrogenation of carbon dioxide catalyzed by $RuX(Y)(PMe_3)_4$.[9] Although the mechanisms of acceleration by water and alcohols were discussed experimentally[9] and theoretically,[8] details of the whole catalytic cycle are still ambiguous, to our knowledge.

* To whom correspondence should be addressed. E-mail: sakaki@moleng.kyoto-u.ac.jp.

[†] Department of Molecular Engineering.

[‡] Fukui Institute for Fundamental Chemistry.

(1) (a) Braunstein, P.; Matt, D.; Nobel, D. *Chem. Rev.* **1988**, *88*, 747. (b) Behr, A. *Angew. Chem., Int. Ed. Engl.* **1988**, *27*, 661. (c) Jessop, P. G.; Ikariya, T.; Noyori, R. *Chem. Rev.* **1995**, *95*, 259. (d) Darensbourg, D. J.; Holtcamp, M. W. *Coord. Chem. Rev.* **1996**, *153*, 155. (e) Walther, D.; Rubens, M.; Rau, S. *Coord. Chem. Rev.* **1999**, *182*, 67.

(2) Inoue, Y.; Izumida, H. Sasaki, S.; Hashimoto, H. *Chem. Lett.* **1976**, 863. Sasaki, S.; Inoue, Y.; Hashimoto, H. *J. Chem. Soc., Chem. Commun.* **1976**, 605.

(3) (a) Darensbourg, D. J.; Ovalles, C. O. *J. Am. Chem. Soc.* **1984**, *106*, 3750. (b) Darensbourg, D. J.; Ovalles, C. O. *J. Am. Chem. Soc.* **1987**, *109*, 3330.

(4) Taqui Khan, M. M.; Halligudi, S. B.; Shukla, S. *J. Mol. Catal.* **1989**, *57*, 47.

(5) Tsai, J. C.; Nicholas, K. H. *J. Am. Chem. Soc.* **1992**, *114*, 5117.

(6) (a) Hutschka, F.; Dedieu, A.; Eichberger, M.; Fornika, R.; Leitner, W. *J. Am. Chem. Soc.* **1997**, *119*, 4432. (b) Hutschka, F.; Dedieu, A. *J. Chem. Soc., Dalton Trans.* **1997**, 1899.

(7) (a) Jessop, P. G.; Ikariya, T.; Noyori, R. J. *Nature* **1994**, *368*, 231. (b) Jessop, P. G.; Hsiano, Y.; Ikariya, T.; Noyori, R. *J. Am. Chem. Soc.* **1994**, *116*, 8851. (c) Jessop, P. G.; Ikariya, T.; Noyori, R. *J. Am. Chem. Soc.* **1996**, *118*, 344.

(8) Yin, C.; Xu, Z.; Yang, S.-Y.; Ng, S. M.; Wong, K. Y.; Lin, Z.; Lau, C. P. *Organometallics* **2001**, *20*, 1216.

(9) Munshi, P.; Main, A. D.; Linehan, J. C.; Tai, C.-C.; Jessop, P. G. *J. Am. Chem. Soc.* **2002**, *124*, 7963.

10.1021/om060307s CCC: $33.50
Publication on Web 06/06/2006

Scheme 1

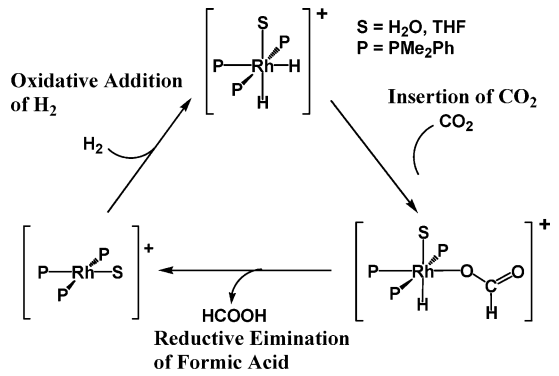

Scheme 2

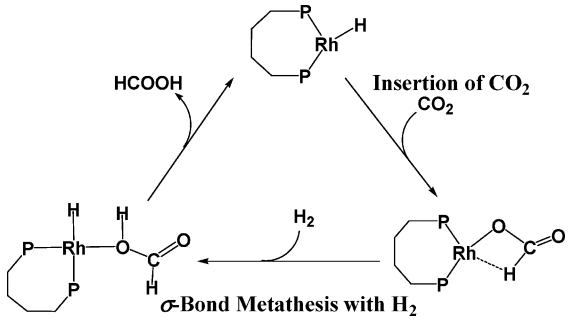

Reaction mechanisms of transition-metal-catalyzed hydrogenation of carbon dioxide have been experimentally and theoretically discussed in the absence of water molecules. For instance, Tsai and his collaborator spectroscopically observed $[RhH(\eta^2\text{-}O_2CH)(PMe_2Ph)_3(S)]^+$ and $[RhH(\eta^1\text{-}O_2CH)(PMe_2Ph)_{3,2}(S)_{1,2}]^+$ (S = solvent such as H_2O or THF) in the catalytic reaction solution and proposed that the hydrogenation of carbon dioxide took place through the insertion of carbon dioxide into the Rh(III)−H bond followed by the reductive elimination of formic acid and the oxidative addition of a dihydrogen molecule to the Rh(I) center to reproduce the active species (see Scheme 1). Our theoretical study presented clear evidence to support this reaction mechanism.[10] Hutschka and his collaborators also theoretically investigated the reaction mechanism of Rh(I)-catalyzed hydrogenation of carbon dioxide and proposed that the hydrogenation took place through the insertion of carbon dioxide into the Rh(I)−H bond followed by the metathesis of the Rh(I) η^1-formate complex with the dihydrogen molecule (Scheme 2).[11] We also theoretically investigated Ru(II)-catalyzed hydrogenation of carbon dioxide and clearly showed that this reaction took place through the insertion of carbon dioxide into the Ru(II)−H bond and the isomerization of a ruthenium(II) η^1-formate intermediate followed by the metathesis of the ruthenium(II) η^1-formate intermediate with a dihydrogen molecule, as shown in Scheme 3.[12] Although the reaction mechanism of transition-metal-catalyzed hydrogenation of carbon dioxide has been theoretically investigated well as described above, all those works devoted attention to the hydrogenation in the absence of water molecules.

The catalytic cycle of the hydrogenation of carbon dioxide in the presence of water molecules has not been investigated

Scheme 3

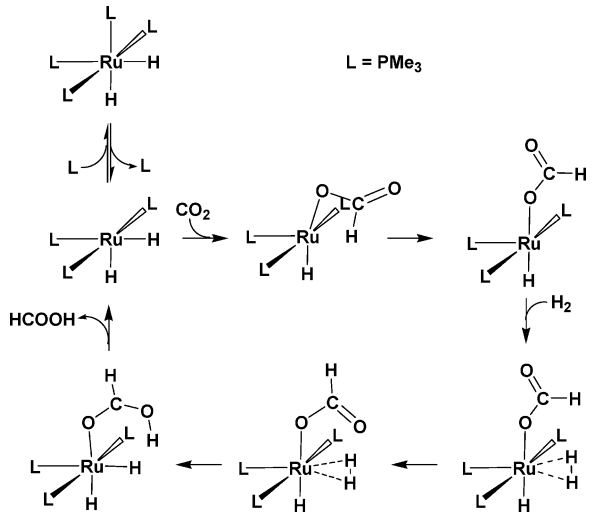

yet, except for only a few theoretical works of a related elementary step.[13,14] One theoretical work with the DFT method reported that water molecules accelerated the insertion of carbon dioxide into the Ru(II)−H bond of $TpRuH(PPh_3)(CH_3CN)$.[13] The reaction of carbon dioxide with $(Cp\text{-}CH_2CH_2NH_2)Ru(H)(diphos)$ was also theoretically investigated with the DFT method.[14] This work reported that not the insertion of carbon dioxide into the Ru(II)−H bond but the H attack to carbon dioxide easily took place because the amine chain accelerated the reaction through a hydrogen-bonding interaction between the H atom of the amine chain and the O atom of carbon dioxide. However, the whole catalytic cycle was not investigated in these works. To clarify the roles of the water molecule, the whole catalytic cycle must be theoretically investigated and each elementary step must be compared with each other.

In this work, we theoretically investigated the Ru(II)-catalyzed hydrogenation of carbon dioxide into formic acid in the presence of water molecules, where the real catalyst, *cis*-$Ru(H)_2(PMe_3)_3$, was employed for calculation. Our purposes here are to clarify the reaction mechanism in the presence of water molecules, to make a comparison between the catalytic cycle in the absence of water molecules and that in the presence of water molecules, and to provide theoretical answers to questions of how and why water molecules accelerate the reaction. Also, we investigated if amine and alcohol accelerated this hydrogenation reaction.

Computational Details

Geometries were optimized with the DFT method, where the B3LYP hybrid functional[15,16] was used for the exchange−correlation term. We ascertained that each optimized transition state exhibited one imaginary frequency and that geometry changes induced by the imaginary frequency were consistent with the reaction course. Energy and population changes were calculated with the DFT and MP2-MP4(SDQ) methods. Solvation effects were evaluated with the DPCM method.[17] The CCSD(T) method was also employed in

(10) Musashi, Y.; Sakaki, S. *J. Am. Chem. Soc.* **2002**, *124*, 7588.
(11) Hutschka, F.; Dedieu, A.; Eichberger, M.; Fornika, R.; Leitner, W. *J. Am. Chem. Soc.* **1997**, *119*, 4432. (b) Hutschka, F.; Dedie, A. *J. Chem. Soc., Dalton Trans.* **1997**, 1899.
(12) (a) Musashi, Y.; Sakaki, S. *J. Am. Chem. Soc.* **2000**, *122*, 3867. (b) Ohnishi, Y.; Matsunaga, T.; Nakao, Y.; Sato, H.; Sakaki, S. *J. Am. Chem. Soc.* **2005**, *127*, 4021.
(13) Yin, C.; Xu, A.; Yang, S.-Y.; Ng, S. M.; Wong, K. Y.; Lin, Z.; Lau, C. P. *Organometallics* **2001**, *20*, 1216.
(14) Matsubara, T. *Organometallics* **2000**, *20*, 19.
(15) (a) Becke, A. D. *Phys. Rev. A* **1988**, *38*, 3098. (b) Becke, A. D. *J. Chem. Phys.* **1993**, *98*, 5648.
(16) Lee, C.; Yang, W.; Parr, R. G.. *Phys. Rev. B* **1988**, *37*, 785.
(17) (a) Miertus, S.; Scrocco, E.; Tomasi, J. *Chem. Phys.* **1981**, *55*, 117. (b) Pascual-Ahuir, J. L.; Silla, E.; Tomasi, J.; Bonaccorsi, R. *J. Comput. Chem.* **1987**, *8*, 778. (c) Floris, F.; Tomasi, J. *J. Comput. Chem.* **1989**, *10*, 616. (d) Tomasi, J.; Persico, M. *Chem. Rev.* **1994**, *94*, 2027.

the most important elementary step to check the reliability of the DFT and MP4(SDQ) methods.

Two kinds of basis set systems were used. In the geometry optimization, the following basis set system (BS-I) was employed: Core electrons of P (up to 2p) and Ru (up to 3d) were replaced with Los Alamos effective core potentials (ECPs),[18] and the valence electrons were represented with (21/21/1) and (341/321/31) basis sets,[19] respectively. For carbon dioxide and the methyl group of trimethylphosphine, 6-31G(d) basis sets were used.[19] For the hydride ligand, dihydrogen molecule, and water molecule, 6-311G(d,p) basis sets[20] were used. Energy changes were calculated with a better basis set system (BS-II), using geometries optimized by the DFT-(B3LYP)/BS-I method. In BS-II, a (541/541/211/1) basis set[18a,21,22] was employed for Ru with the same ECPs as those of BS-I. For the hydride ligand, dihydrogen molecule, water molecule, carbon dioxide, and formate anion, the cc-pVDZ basis sets were employed,[23] where a d-polarization function was added to each atom and a diffuse function was added to the O atom (aug-cc-pVDZ). For P, the same basis set and ECPs as those of BS-I were used. For the methyl group of trimethylphosphine, 6-31G basis sets were used in order to reduce the computational cost of the MP4(SDQ) calculations.

We evaluated the free energy change in two ways as in our previous works.[12b,24] In one way, translation, rotation, and vibration movements were considered to evaluate entropy and thermal energy, where all substrates were treated as ideal gases. We evaluated the entropy effects under the typical reaction conditions, where the pressures of H_2 and CO_2 were 80 and 120 atm, respectively, and the temperature was 323.15 K. The DFT/BS-I method was used to calculate vibration frequencies without a scaling factor. In the other way, vibration movements were considered in the evaluation of entropy but neither translation movements nor rotation ones were considered, since this reaction was carried out in supercritical carbon dioxide solvent, in which the translation and rotation movements are considerably suppressed, unlike those in an ideal gas. The free energy change estimated in this way is named ΔG_v hereafter. In the former estimation method, entropy significantly decreases when two molecules form an adduct, as expected. In the latter estimation method, on the other hand, the entropy change is small, as will be discussed below. The former method apparently overestimates entropy and thermal energy changes of the solution reaction, because translation and rotation movements are considerably suppressed in solution. On the other hand, the latter one underestimates entropy and thermal energy changes because translation and rotation movements are not completely frozen in solution. A true value of free energy change would be intermediate between the ΔG value evaluated by the former method and the ΔG_v value by the latter one. Because this ambiguity remains in the estimation of entropy and thermal energy changes, we will discuss each elementary step with the usual potential energy changes and then discuss it with the free energy changes evaluated in these two ways.

Scheme 4

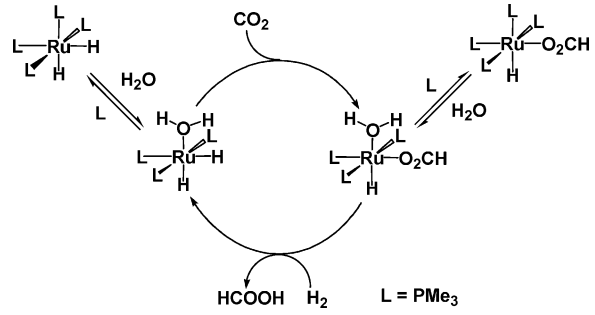

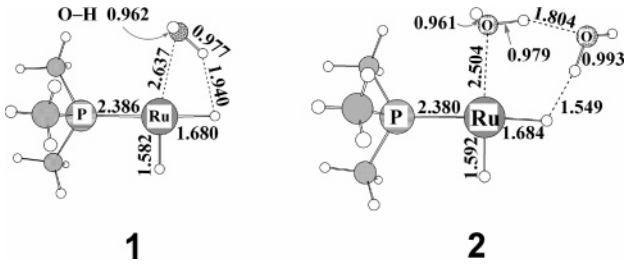

Figure 1. Geometries of *cis*-$Ru(H)_2(PMe_3)_3(H_2O)$ and *cis*-$Ru(H)_2(PMe_3)_3(H_2O)_2$. Bond lengths are in angstroms and bond angles in degrees. Two PMe_3 ligands above and below the Ru center are omitted in all the figures to show clearly the geometry changes by the reaction.

Scheme 5

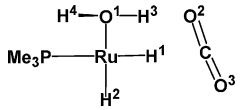

The Gaussian 98 program package was used for these calculations.[25] Population analysis was carried out with the method of Weinhold et al.[26] Molecular orbitals were drawn with the MOLEKEL program package.[27]

Results and Discussion

Hydride Migration from the Ru(II) Center to CO_2. *cis*-$RuH_2(PMe_3)_3(H_2O)$ was experimentally proposed to be formed from *cis*-$RuH_2(PMe_3)_4$ as an active species in the presence of water molecules,[7c] as shown in Scheme 4. Because *cis*-$RuH_2(PMe_3)_4$ is a six-coordinate complex, it is likely that associative substitution of PMe_3 for H_2O does not occur easily. In dissociative substitution, *cis*-$RuH_2(PMe_3)_3$ is formed first, in which a vacant site is at a position trans to H because of the strong trans influence of the H(hydride) ligand. Then, H_2O approaches the Ru center at the vacant site to form $Ru(H)_2(PMe_3)_3(H_2O)$, **1**. In **1**, the H_2O moiety tilts toward the H^1 ligand, as shown in Figure 1, because the H^3 atom of H_2O is drawn to the H^1 ligand by the proton−hydride (H^3-H^1) electrostatic interaction, where H^1, H^2, etc. are defined in Scheme 5; the NBO net charge is $-0.205e$ for H^1 and $+0.511e$ for H^3. This distorted $Ru-OH_2$ coordinate bond is weaker than the usual $Ru-OH_2$ coordinate bond with normal coordination structure, because the overlap between the lone pair orbital of H_2O and the empty d_σ orbital of Ru is smaller in this geometry than that

(18) (a) Hay, P. J.; Wadt, W. R. *J. Chem. Phys.* **1985**, *82*, 299. (b) Wadt, W. R.; Hay, P. J. *J. Chem. Phys.* **1985**, *82*, 284. (c) Höllwarth, A.; Böhme, M.; Dapprich, S.; Ehlers, A. W.; Gobbi, A.; Jonas, V.; Köhler, K. F.; Stegmann, R.; Veldkamp, A.; Frenking, G. *Chem. Phys. Lett.* **1993**, *208*, 237.

(19) Hehre, W. J.; R. Ditchfield, R.; Pople, J. A. *J. Chem. Phys.* **1972**, *56*, 2257.

(20) Krishnan, R.; Binkley, J. S.; Seeger, R.; Pople, J. A. *J. Chem. Phys.* **1980**, *72*, 650.

(21) Couty, M.; Hall, M. B. *J. Comput. Chem.* **1996**, *17*, 1359.

(22) Ehlers, A. W.; Böhme, M.; Dapprich, S.; Gobbi, A.; Höllwarth, A.; Jonas, V.; Köhler, K. F.; Stegmann, P.; Veldkamp, A.; Frenking, G. *Chem. Phys. Lett.* **1993**, *208*, 111.

(23) Dunning, T. H., Jr. *J. Chem. Phys.* **1989**, *90*, 1007.

(24) (a) Tamura, H.; Yamazaki, H.; Sato, H.; Sakaki, S. *J. Am. Chem. Soc.* **2003**, *125*, 16114. (b) Sakaki, S.; Takayama, T.; Sumimoto, M.; Sugimoto, M. *J. Am. Chem. Soc.* **2004**, *126*, 3332. (c) Sumimoto, M.; Iwane, N.; Takayama, T.; Sakaki, S. *J. Am. Chem. Soc.* **2004**, *126*, 10457.

(25) Pople, J. A.; et al. *Gaussian 98, version A.11.3*; Gaussian Inc.: Pittsburgh, PA, 1998.

(26) Reed, A. E.; Curtis, L. A.; Weinhold, F. *Chem. Rev.* **1988**, *88*, 849, and references therein.

(27) Flükiger, P.; Lüthi, H. P.; Portann, S.; Weber, J. *MOLEKEL v.4.3* for Scientific Computing; Manno, Switzerland, 2000−2002. Portman, S.; Lüthi, H. P. *Chimia* **2000**, *54*, 766.

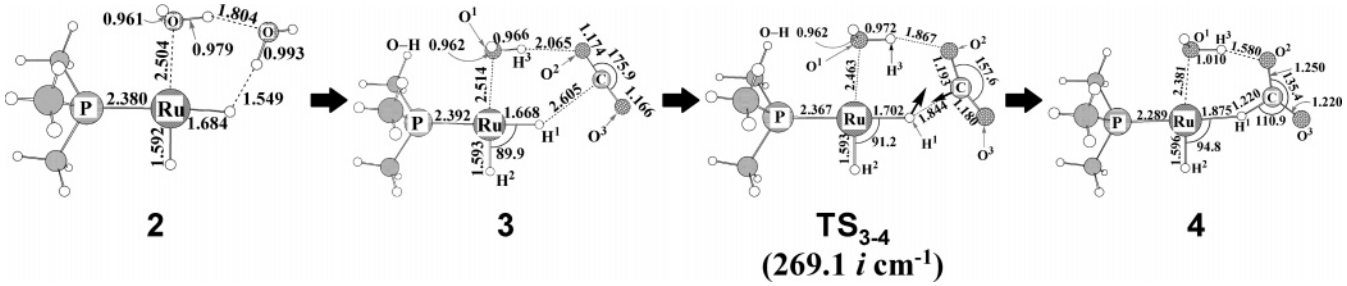

Figure 2. Geometry changes by the nucleophilic attack of the hydride ligand to the C center of carbon dioxide in *cis*-$Ru(H_2)(PMe_3)_3(H_2O)(CO_2)$. Bond lengths are in angstroms and bond angle in degrees. In parentheses is the imaginary frequency. Arrows in $\mathbf{TS_{3-4}}$ represent important movements of nuclei in the transition state.

in the normal coordinate structure. Since it is likely that water molecules form a cluster in hydrophobic supercritical carbon dioxide, we investigated the possibility that a cluster of two water molecules binds with the Ru complex to afford $Ru(H)_2(PMe_3)_3(H_2O)_2$, **2**. In **2**, the six-membered ring structure that consists of Ru and two H_2O molecules distorts little, as shown in Figure 1; one H_2O interacts with the H^1 ligand, keeping the hydrogen bond with the H_2O ligand that coordinates with the Ru center in a normal coordination structure. Formation of **2** yields a larger stabilization energy than formation of **1**, as shown in eqs 1a and 1b, where the stabilization energy was evaluated with the MP4(SDQ)/BS-II method.

$$Ru(H)_2(PMe_3)_3 + H_2O \rightarrow Ru(H)_2(PMe_3)_3(H_2O),\ \mathbf{1}$$
$$\Delta E = -13.6\ \text{kcal/mol} \quad (1a)$$

$$Ru(H)_2(PMe_3)_3 + (H_2O)_2 \rightarrow Ru(H)_2(PMe_3)_3(H_2O)_2,\ \mathbf{2}$$
$$\Delta E = -24.5\ \text{kcal/mol} \quad (1b)$$

In the next step, CO_2 approaches **2** to form a precursor complex, *cis*-$RuH_2(PMe_3)_3(H_2O)(CO_2)$, **3**, through substitution of H_2O for CO_2, as shown in Figure 2. In **3**, the six-membered ring that consists of Ru, H_2O, and CO_2 distorts little, like **2**. It is noted that the H^3-O^2 distance (2.065 Å) is much shorter than the H^1-C distance (2.605 Å). This short H^3-O^2 distance suggests that **3** is mainly formed by the H^3-O^2 hydrogen-bonding interaction. The OCO bond angle is 175.9° and the $C-O^2$ and $C-O^3$ bond distances are 1.174 and 1.166 Å, respectively, which are almost the same as those of free CO_2. These geometrical parameters are consistent with the small binding energy of CO_2 with the Ru complex, as will be discussed below.

Starting from **3**, CO_2 approaches the H^1 ligand to afford a formate adduct, $Ru(H)(HCO_2)(H_2O)(PMe_3)_3$, **4** through the transition state $\mathbf{TS_{3-4}}$. In $\mathbf{TS_{3-4}}$, the OCO bond angle decreases to 157.6°, and $C-O^2$ and $C-O^3$ distances increase to 1.193 and 1.180 Å, respectively. The H^2-C distance shortens to 1.844 Å, and the $Ru-H^1$ bond lengthens to 1.702 Å. In the imaginary frequency, the H^1 ligand is approaching the C center of CO_2 and the C center is also approaching the H^1 ligand, as shown by arrows in $\mathbf{TS_{3-4}}$ of Figure 2. These geometrical features suggest that the hydride (H^1) ligand attacks the C center of CO_2. In **4**, the H^1-C distance is 1.220 Å, which is considerably longer than the usual C−H bond (1.160 Å) of the formate anion. This indicates that the C−H bond of formate forms an agostic interaction with the Ru center, because the H atom of formate is negatively charged and the empty d_σ orbital expands toward the H atom of formate. Interestingly, the rather short distance (1.580 Å) between the H^3 atom of H_2O and the O^2 atom of formate clearly shows that the hydrogen bond between these two atoms becomes stronger in **4** than in **3**. The hydrogen bond and the agostic interaction will be discussed below in more detail. It should be noted here that this reaction from **3** to **4** is quite different from the usual CO_2 insertion into the metal−hydride bond, as follows: The C and O atoms of CO_2 do not coordinate with the Ru center in the reactant **3** and the O atom of formate does not interact with the Ru center in the product **4**; remember that in the absence of water molecules CO_2 coordinates with the Ru center and the CO_2 insertion into the Ru−H bond takes place to afford the Ru-(η^1-OCOH) intermediate in which the O atom of formate coordinates with the Ru center.[12b]

Table 1. Energy Change (ΔE_1) of the Adduct Formation of Carbon Dioxide with *cis*-$Ru(H)_2(PR_3)_3(H_2O)_2$, the Activation Barrier (E_a), and the Reaction Energy (ΔE_2) of the Nucleophilic Attack of Hydride to Carbon Dioxide in *cis*-$Ru(H)_2(PR_3)_3(H_2O)(CO_2)$[a]

	R = Me			R = H[b]		
method	ΔE_1	E_a	ΔE_2	ΔE_1	E_a	ΔE_2
MP2	7.6	10.8	6.8	8.0	13.6	19.0
MP3	8.2	10.9	−1.5	8.4	13.6	10.3
MP4(D)	7.6	10.9	2.9	7.9	13.6	14.7
MP4(DQ)	7.2	11.4	3.9	7.5	14.1	15.7
MP4(SDQ)	7.3	10.6	3.3	7.7	13.4	15.0
CCSD				7.9	13.4	12.3
CCSD(T)				8.3	12.6	12.2
DFT(B3LYP)	9.0	11.0	3.6	8.8	13.8	13.0
PCM(*n*-heptane)[c]	9.8	11.1	−1.2			
PCM(THF)[c]	9.2	10.8	−5.7			

[a] ΔE_1, E_a, and ΔE_2 represent the relative energy of **3** to **2**, that of $\mathbf{TS_{3-4}}$ to **2**, and that of **4** to **2**, respectively. These values were calculated by the MP2-MP4(SDQ), CCSD, CCSD(T), and DFT(B3LYP)/BS-II methods (kcal/mol). [b] In the single-point calculation of R = H, the geometry was taken to be the same as that of R = Me, where the P−H bond length was fixed to 1.430 Å, which is an optimized value of free PH_3. [c] The PCM calculations were carried out with the DFT(B3LYP)/BS-II method.

Energy changes of the reaction from **2** to **4** are calculated with various methods, as shown in Table 1. Both the DFT and MP2 to MP4(SDQ) calculations indicate that the substitution of H_2O for CO_2 is moderately endothermic, which means that the interaction between CO_2 and $Ru(H)_2(PMe_3)_3(H_2O)$ is not sufficiently strong. A similar activation barrier (E_a) is calculated with all these computational methods. Although the reaction energy considerably fluctuates at the MP2 and MP3 levels, it converges upon going from MP3 to MP4(SDQ), and the DFT-calculated reaction energy is almost the same as the MP4(SDQ)-calculated value. Also, we applied the CCSD(T) method to this reaction, where PMe_3 was replaced with PH_3 because $Ru(H)_2(PMe_3)_3(H_2O)(CO_2)$ was too large to perform the CCSD(T) calculation. As shown in Table 1, the DFT, MP2 to MP4(SDQ), and CCSD(T) methods present similar activation barriers, and the DFT-calculated reaction energy is almost the same as the CCSD(T)-calculated value. Although the MP4(SDQ)-calculated reaction energy is moderately larger than the CCSD(T)- and

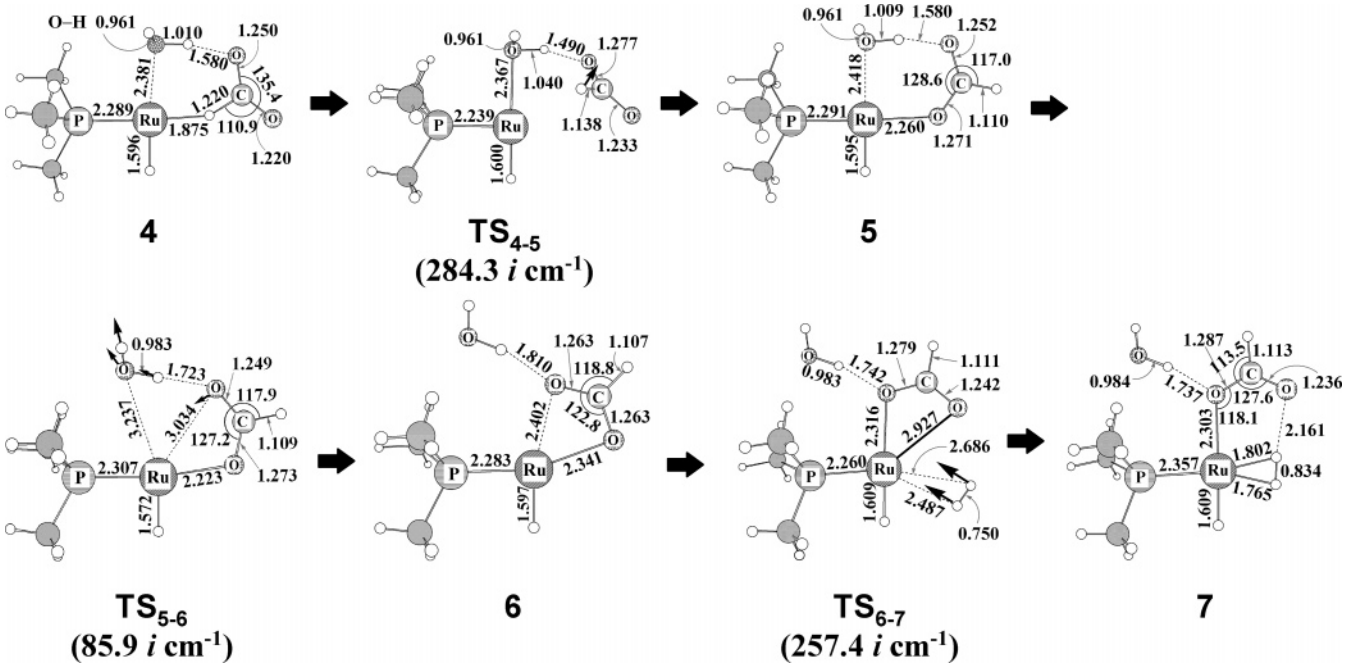

Figure 3. Geometry changes by the isomerization of the formate moiety in *cis*-Ru(H)(PMe_3)$_3$(OCOH)(H_2O) followed by coordination of a dihydrogen molecule to the Ru center. Bond lengths are in angstroms and bond angles in degrees. In parentheses are the imaginary frequencies. Arrows in $\mathbf{TS_{4-5}}$, $\mathbf{TS_{5-6}}$, and $\mathbf{TS_{6-7}}$ represent important movements of nuclei in these transition states.

DFT-calculated values, the difference between them is not large. These results indicate that the DFT and MP4(SDQ) methods present reliable energy changes here. The endothermicity of this reaction is evaluated to be 3.3 and 3.6 kcal/mol with the MP4(SDQ) and DFT methods, respectively.[28] Interestingly, the activation barrier of the hydride attack is considerably smaller than that (16.1 kcal/mol) of the usual CO_2 insertion reaction into the Ru−H bond; in other words, this hydride attack occurs much more easily than the usual CO_2 insertion into the Ru−H bond. Also, it should be noted that the former is slightly endothermic ($\Delta E = 3.3$ kcal/mol), but the latter is considerably endothermic ($\Delta E = 18.1$ kcal/mol). These results directly relate to the acceleration by water molecules, as will be discussed below in more detail.

Solvent effects were investigated with the DPCM method, where we employed parameters of *n*-heptane to mimic the hydrophobic atmosphere of supercritical carbon dioxide, as in our previous work,[12b] and those of THF to make a comparison between nonpolar and polar solvents. The activation barrier is little different in the gas phase, *n*-heptane, and THF, while the reaction energy considerably changes; although the nucleophilic attack is endothermic in the gas phase, it becomes slightly exothermic in *n*-heptane and moderately exothermic in THF. The small solvent effect on the activation barrier is interpreted in terms of the reactant-like transition state. The increase in exothermicity by a polar solvent is easily understood by considering that the product **4** is more polar than the reactant **2**. Thus, it is concluded that the polar solvent accelerates this nucleophilic attack and that this nucleophilic attack becomes exothermic (much less endothermic, at least) in supercritical carbon dioxide.

Isomerization of the Formate Moiety in Ru(H)(OCOH)(H_2O)(PMe_3)$_3$ Followed by Coordination of a Dihydrogen Molecule. In **4**, the O and H atoms of formate interact with the aqua ligand through the hydrogen bond and with the Ru center through an agostic interaction, respectively, whereas the formate anion usually coordinates with the metal center through the negatively charged O atom. Thus, **4** is not very stable and the rotational isomerization of the formate anion easily takes place around the C−O bond to afford the usual η^1-formate complex Ru(H)(η^1-OCOH)(H_2O)(PMe_3)$_3$, **5**, through $\mathbf{TS_{4-5}}$, as shown in Figure 3. The activation barrier is moderate; it is 6.7 and 6.4 kcal/mol by the DFT and MP4(SDQ) calculations, respectively, as shown in Table 2A. It is noted that this rotational isomerization is considerably exothermic: 17.1 and 22.8 kcal/mol by the DFT and MP4(SDQ) calculations, respectively. In **5**, it is also noted that the H^3-O^2 distance between the aqua and the formate ligands changes little from that of **4**, which clearly shows that the hydrogen bond between the aqua and the formate ligands in **5** is as strong as that in **4**. Thus, the small activation barrier and the large exothermicity mainly come from the formation of the strong Ru−(η^1-OCOH) bond and the breaking of the weak agostic interaction between the C−H bond and the Ru center. The solvent effects are not significantly large, as shown in Table 2A; the activation barrier moderately increases in the order gas phase < *n*-heptane < THF, and the exothermicity moderately decreases in the order gas phase > *n*-heptane > THF. This is easily interpreted as follows: two negatively charged O atoms take positions distant from the Ru center in **4**, but one of them coordinates with the Ru center in **5**; in other words, the polarity decreases upon going to **5** from **4**.

Because the formate anion usually coordinates with the metal center as a bidentate ligand, we optimized the Ru-(η^2-formate) complex **6**, in which one water molecule was added to **6** to balance with **5**. The water molecule interacts with the O atom of η^2-formate through a hydrogen-bonding interaction. Inter-

(28) (a) The DFT method presented much a smaller activation barrier (5.6 kcal/mol) and endothermicity (6.5 kcal/mol) than does the MP4(SDQ) method. The activation barrier considerably fluctuates at the MP2 and MP3 levels but seems to converge upon going to MP4(SDQ) from MP3 (see ref 12b and Supporting Information Figure S1). The small activation barrier by the DFT calculation results from the underestimation of the stabilization energy of the CO_2 complex Ru($H)_2$(PMe_3)$_3$(CO_2). Our recent theoretical work[28b] clearly shows that the binding energy of the π-conjugate system with the transition-metal complex is underestimated by the DFT method. Thus, we employed here the MP4(SDQ)-evaluated energy change for the CO_2 insertion step. (b) Kameno, Y.; Ikeda, A.; Nakao, Y.; Sato, H.; Sakaki, S. *J. Phys. Chem. A* **2005**, *109*, 8055.

Table 2. Activation Barriers and Reaction Energies[a] of the Isomerization Reaction from Ru(H)(η^1-HCOO)(H_2O)(PMe_3)$_3$, 4, to Ru(H)(η^1-OCOH)(H_2O)(PMe_3)$_3$, 5, and that from 5 to Ru(H)(η^2-O_2CH)(PMe_3)$_3$(H_2O), 6

(A) Reaction from **4** to **5**

method	E_a	ΔE
MP2	6.7 (6.8)[b]	−21.3(−20.0)[b]
MP3	3.7 (3.8)	−25.2 (−23.8)
MP4(D)	5.5 (5.6)	−23.4 (−22.1)
MP4(DQ)	5.4 (5.5)	−23.7 (−22.3)
MP4(SDQ)	6.4 (6.5)	−22.8 (−21.4)
DFT(B3LYP)	6.7 (6.8)	−17.1 (−16.7)
PCM(*n*-heptane)[c]	7.3	−15.8
PCM(THF)[c]	8.8	−14.7

(B) Reaction from **5** to **6**

method	E_a	ΔE
MP2	7.5 (6.7)[b]	0.4 (−0.5)[b]
MP3	6.8 (6.0)	1.6 (0.7)
MP4(D)	7.1 (6.3)	1.0 (0.1)
MP4(DQ)	6.8 (6.0)	0.7 (−0.2)
MP4(SDQ)	7.2 (6.4)	0.5 (−0.5)
DFT(B3LYP)	4.5 (3.7)	0.0 (−1.0)
PCM(*n*-heptane)[c]	6.3	2.3
PCM(THF)[c]	9.2	5.5

[a] These values are calculated by the MP2-MP4(SDQ) and DFT(B3LYP)/BS-II methods (kcal/mol). [b] With correction of zero-point energy. [c] The PCM calculations were carried out with the DFT(B3LYP)/BS-II method.

mediate **5** converts to **6** through the transition state $\mathbf{TS_{5-6}}$ with a moderate activation barrier of 4.5 and 7.2 kcal/mol from the DFT and MP4(SDQ) calculations, respectively, as shown in Table 2B. Interestingly, **6** is as stable as **5**, whereas the η^2-formate ligand more strongly coordinates with the Ru center in **6** than does the η^1-formate ligand. This is interpreted as follows: The Ru−O bond of the Ru-(η^1-formate) complex is stronger than the Ru−O bond of the Ru-(η^2-formate) complex, as clearly shown by the Ru−O^3 bond of **5** being shorter than that of **6** by 0.08 Å. Thus, the Ru−OH_2 bond and one strong Ru−O bond of **5** compensate well two Ru−O bonds of **6**. As a result, **6** is as stable as **5**. Solvent effects are somewhat large here. The activation barrier and endothermicity considerably increase in the order gas phase < *n*-heptane < THF. This is because one negatively charged O atom coordinates with the Ru center in **5**, but two negatively charged O atoms coordinate with the Ru center in **6**; in other words, the polarity of the reaction system decreases upon going to **6** from **5**.

The next step is the coordination of a dihydrogen molecule with **6**. The dihydrogen molecule approaches the Ru center from the right-hand side in Figure 3, to afford the dihydrogen complex Ru(H)(η^1-OCOH)(H_2)(PMe_3)$_3$(H_2O), **7**, through the transition state $\mathbf{TS_{6-7}}$. The geometry of **7** is essentially the same as that of the previously reported dihydrogen complex Ru(H)(η^1-OCOH)(H_2)(PH_3)$_3$;[12b] the distances between the Ru center and the H atom are 1.802 and 1.765 Å, and the H−H distance (0.834 Å) is much longer than the equilibrium distance (0.744 Å by the DFT/BS-I calculation). These geometrical features indicate that the dihydrogen molecule strongly coordinates with the Ru center. This **6** → **7** reaction requires a somewhat large activation barrier because the Ru−O^3 bond should be broken in this reaction; the barrier is calculated to be 7.3 kcal/mol with the DFT method and 8.1 kcal/mol with the MP4(SDQ) method, as shown in Table 3A. The energy of the reaction is −6.6 kcal/mol in the DFT calculation and −7.6 kcal/mol in the MP4(SDQ) calculation. The reaction energy moderately fluctuates at the MP2 and MP3 levels but converges upon going to MP4(SDQ) from MP3, suggesting that the MP4(SDQ) method presents a reliable binding energy of the dihydrogen molecule.

Table 3. Activation Barriers and Reaction Energies[a] of the Coordination of a Dihydrogen Molecule to the Ruthenium Center (6 → 7) and the Metathesis Reaction (7 → 8)

(A) Reaction from **6** to **7**

method	E_a	ΔE
MP2	8.7 (11.9)[b]	−9.8 (−4.7)[b]
MP3	6.9 (10.1)	−7.3 (−2.1)
MP4(D)	7.8 (10.9)	−8.1 (−3.0)
MP4(DQ)	7.8 (11.0)	−8.1 (−3.0)
MP4(SDQ)	8.1 (11.2)	−7.6 (−2.4)
DFT(B3LYP)	7.3 (10.4)	−6.6 (−1.5)
PCM(*n*-heptane)[c]	6.6	−8.0
PCM(THF)[c]	6.0	−8.8

(B) Reaction from **7** to **8**

method	E_a	ΔE
MP2	12.4 (10.6)[b]	12.9 (12.8)[b]
MP3	16.1 (14.3)	17.0 (16.8)
MP4(D)	13.7 (11.9)	13.8 (13.7)
MP4(DQ)	13.5 (11.8)	13.2 (13.0)
MP4(SDQ)	13.2 (11.4)	13.2 (13.0)
DFT(B3LYP)	9.0 (7.3)	9.3 (9.2)
PCM(*n*-heptane)[c]	10.2	10.3
PCM(THF)[c]	11.2	10.3

[a] These values are calculated by the MP2-MP4(SDQ) and DFT(B3LYP)/BS-II methods (kcal/mol). [b] With correction of zero-point energy. [c] The PCM calculations were carried out with the DFT(B3LYP)/BS-II method.

Solvation effects are moderate in this process. The activation barrier slightly decreases in the order gas phase > *n*-heptane > THF, and the exothermicity moderately increases in the order gas phase < *n*-heptane < THF. This is because the η^2-formate moiety changes to the η^1-formate moiety upon going to **7** from **6**; in other words, this is the reverse of the conversion of **5** to **6**.

Because two molecules participate in this elementary step to form one adduct, the entropy effect should be considered. The $\Delta G^{\ddagger}$ and $\Delta G_v^{\ddagger}$ values are estimated to be 16.0 and 10.9 kcal/mol based on DFT-calculated potential energy changes and 16.8 and 11.7 kcal/mol based on the MP4(SDQ)-calculated potential energy changes. If we adopt the $\Delta G^{\ddagger}$ value in gas phase, this step becomes rate-determining. If we adopt the $\Delta G_v^{\ddagger}$ value without contributions from translation and rotation movements, the metathesis becomes the rate-determining step. These issues will be discussed below in detail.

Of course, we must consider the possibility that the dihydrogen coordination with the Ru center occurs in **5** without conversion to **6**. This reaction course does not participate in the catalytic cycle, as will be discussed below (Scheme 9).

Metathesis of Dihydrogen Molecules with the Ru-(η^1-OCOH) Complex. Starting from **7**, the metathesis of the Ru-(η^1-OCOH) moiety with a dihydrogen molecule proceeds through $\mathbf{TS_{7-8}}$,[30] to form Ru(H)$_2$(PMe_3)$_3$(HCOOH), **8**, in which the formic acid coordinates with the Ru center, as shown in Figure 4. The geometry changes by the metathesis are essentially the same as those of the metathesis in the absence of water molecules,[12b] except for the presence of a water molecule interacting with formic acid through a hydrogen-bonding interaction. As the metathesis proceeds, the O−H distance between water and formic acid becomes longer, which indicates that the hydrogen bond becomes weaker in the reaction. This is because the O^3 atom of **7** is negatively charged in a formal sense, but it becomes neutral in **8**. As a result, the activation

(29) (a) Similar orbital mixing was reported previously.[29b] (b) Sakaki, S.; Aizawa, T.; Koga, N.; Morokuma, K.; Ohkubo, K. *Inorg. Chem.* **1989**, *28*, 103. Sakaki, S.; Ohkubo, K. *Inorg. Chem.* **1989**, *28*, 2583. Sakaki, S. *J. Am. Chem. Soc.* **1992**, *114*, 2055.

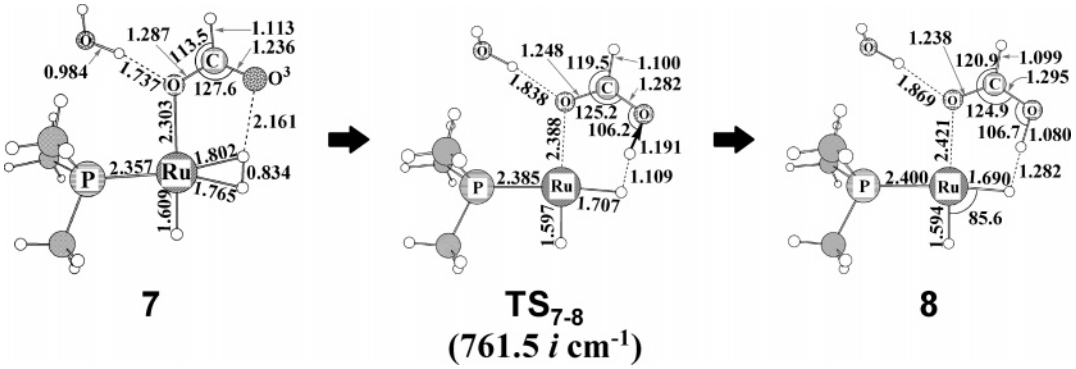

Figure 4. Geometry changes by the metathesis of *cis*-Ru(H)(PMe_3)$_3$(η^1-OCOH)(H_2O). In parentheses is the imaginary frequency. Arrows in $\mathbf{TS_{7-8}}$ represent important movements of nuclei in this transition state.

barrier of the metathesis is moderately larger in the presence of water molecules than that in the absence of water molecules, as shown in Table 3B; it is calculated to be 9.0 and 13.2 kcal/mol with the DFT and the MP4(SDQ) methods, respectively, in the presence of water molecules and 4.9 and 9.0 kcal/mol with the DFT and the MP4(SDQ) methods, respectively, in the absence of water molecules. In this step, somewhat large differences between the DFT and MP4(SDQ) methods are observed in the activation barrier and reaction energy. Both activation barrier and reaction energy considerably fluctuate at the MP2 and MP3 levels, but they converge upon going to MP4(SDQ) from MP3. Here, we adopted MP4(SDQ)-calculated energy changes.

The activation barrier and the endothermicity moderately increase in the order gas phase < *n*-heptane < THF. The discussion is omitted here because it was discussed in our previous work.[12b]

Energy Changes along the Whole Catalytic Cycle. Energy changes along the whole catalytic cycle are shown in Figure 5, where the correction of the zero-point energy is made in Figure 5; note that the values in Figure 5 are different from those of Tables 1−3 because the correction of zero-point energy was not made in those tables. In the absence of water molecules, the Ru-(η^1-OCOH) intermediate is produced by the usual CO_2 insertion into the Ru−H bond, which occurs with a considerably large activation barrier of 17.6 kcal/mol and endothermicity of 21.7 kcal/mol,[12b] where the MP4(SDQ)-calculated values are given.[28] On the other hand, when water molecules are present, the H attack to CO_2 easily takes place with a very small activation barrier of 3.4 (2.1) kcal/mol and exothermicity of 1.6 (2.9) kcal/mol to afford **4**, where the MP4(SDQ)- and DFT-calculated values are given without parentheses and in parentheses, respectively, hereafter. If we take **2** as a standard (because **3** is less stable than **2**), then the activation barrier and the endothermicity increase to 9.3 (9.7) and 4.3 (4.7) kcal/mol, respectively. It should be noted that the isomerization of the OCOH moiety easily takes place in **4** with an activation barrier of 6.5 (6.8) kcal/mol and the considerably large exothermicity of 21.4 (15.7) kcal/mol to afford the stable intermediate Ru(H)(η^1-OCOH)(H_2O)(PMe_3)$_3$, **5**. Because this intermediate is very stable, the back reaction does not occur. In the absence of water molecules, on the other hand, the coordination of a dihydrogen molecule with Ru(H)(η^1-OCOH)(PMe_3)$_3$ must occur to suppress the back reaction because the CO_2 insertion into the Ru−H bond is considerably endothermic;[12b] in other words, the deinsertion of CO_2 more easily occurs with a smaller activation barrier than the CO_2 insertion if the dihydrogen molecule does not coordinate with the Ru center. However, the coordination of the dihydrogen molecule is a bimolecular process, but the isomerization of **4** is a unimolecular process. Moreover, the concentration of dihydrogen molecules is not sufficiently large under the reaction conditions; remember that the yield of formic acid increases with an increase in the dihydrogen pressure.[7b] Thus, the isomerization of **4** more easily takes place than the coordination of a dihydrogen molecule with Ru(H)(η^1-OCOH)(PMe_3)$_3$. These results are summarized as follows: (1) A water molecule suppresses the usual CO_2 insertion, which is considerably endothermic. (2) The nucleophilic attack of the H ligand to CO_2 easily takes place to afford the ruthenium(II) hydride η^1-formate intermediate **5**, the reason for which will be discussed below in detail. (3) The thus-formed **5** is extremely stable, and therefore, the back reaction from **5** to **2** does not occur easily.

The next step is the isomerization of the η^1-formate intermediate **5** to the η^2-formate intermediate **6**, the activation barrier of which is calculated to be 6.3 (3.6) kcal/mol. The coordination of a dihydrogen molecule with **6** needs a moderate activation barrier of 11.2 (10.4) kcal/mol. The final step is the metathesis, the activation barrier of which is 11.4 (7.3) kcal/mol. From these results, the rate-determining step is either the metathesis or the coordination of the dihydrogen molecule. Both activation barriers are smaller than that (17.6 kcal/mol) of the CO_2 insertion into the Ru−H bond, which is the rate-determining step in the absence of a water molecule. Thus, the presence of a water molecule changes the rate-determining step and considerably decreases the activation barrier of the rate-determining step; in other words, the hydrogenation of carbon dioxide is accelerated very much by the presence of water molecules.

We wish to mention here the ΔG surface. The activation free energy change $\Delta G^{\ddagger}$ is little different from the potential energy change in the H attack to CO_2 and the metathesis of **7**, because these two steps are unimolecular processes. However, the $\Delta G^{\ddagger}$ value for the coordination of the dihydrogen molecule is 16.8 (16.0) kcal/mol, being much larger than the potential energy change because the coordination of a dihydrogen molecule is a

(30) The product **8** is calculated to be slightly more stable than the transition state $\mathbf{TS_{7-8}}$ by 0.3 kcal/mol with the DFT/BS-I method, while **8** is calculated to have almost the same energy as $\mathbf{TS_{7-8}}$ with the MP4(SDQ)/BS-II method. However, the zero-point energy correction destabilizes **8** in energy more than $\mathbf{TS_{7-8}}$, and as a result, **8** becomes slightly less stable than $\mathbf{TS_{7-8}}$, as shown in Figure 5, although the energy difference is very small. The smaller zero-point energy of $\mathbf{TS_{7-8}}$ than that of **8** arises from the fact that the O−H stretching of the formate moiety contributes to the zero-point energy of **8** but little to that of $\mathbf{TS_{7-8}}$ because the O−H stretching is mainly involved in the imaginary frequency. $\mathbf{TS_{7-8}}$ is considered reasonable from the geometry and the geometry changes in imaginary frequency. Although **8** has almost the same energy as $\mathbf{TS_{7-8}}$, amine was added to the solution in excess under real experimental conditions to stabilize the product by formation of an adduct with formic acid. Thus, the similar stabilities of **8** and $\mathbf{TS_{7-8}}$ are not unreasonable.

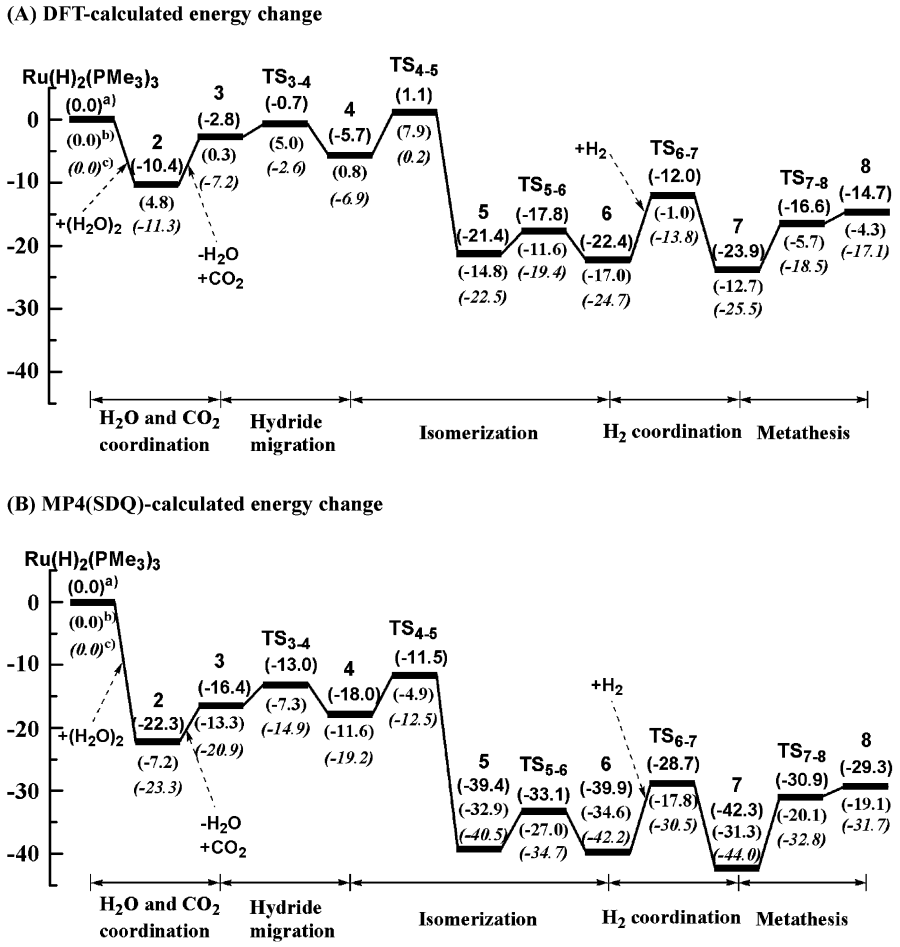

Figure 5. Potential energy change and free energy change (kcal/mol unit) along the catalytic cycle. (a) Potential energy change with zero-point energy correction. (b) In the ΔG value, contributions of translation, rotation, and vibration movements are considered. (c) In the ΔG_v value, contributions of vibration movements are considered, while those of translation and rotation movements are neglected.

bimolecular process. This value is similar to the $\Delta G^{\ddagger}$ value of the CO_2 insertion, which is the rate-determining step in the absence of water molecules. However, we must remember that the translation and rotation movements are considerably suppressed in supercritical carbon dioxide compared to those in an ideal gas. This means that the decrease in entropy by the coordination of a dihydrogen molecule is overestimated here. If we assume that translation and rotation movements are completely suppressed, the activation free energy change is given by the $\Delta G_v^{\ddagger}$ value. This value is almost the same as the potential energy change and much smaller than the $\Delta G^{\ddagger}$ value. The true value of the free energy change is between these two values. Summarizing these results, the conclusions are presented as follows: (1) The activation free energy change of the dihydrogen coordination step (**6** → **7**) is smaller than 16.8 (16.0) kcal/mol (see above and Figure 5), i.e., smaller than that of the CO_2 insertion. (2) The activation free energy change of this step (**6** → **7**) could be larger than 11.7 (10.9) kcal/mol, which is almost the same as the $\Delta G^{\ddagger}$ value of the metathesis (**7** → **8**), 11.2 (7.0) kcal/mol (see above and Figure 5). (3) Thus, the dihydrogen coordination step (**6** → **7**) is rate-determining in the presence of water molecules. (4) Because its activation free energy change is smaller than that of the CO_2 insertion, the reaction is accelerated by the presence of water molecules in the free energy surface, too.

At the end of this section, we wish to mention the solvent effects on the whole catalytic cycle. The activation barrier of the dihydrogen coordination step moderately decreases in the order gas phase > *n*-heptane > THF, while the activation barrier of the metathesis increases in the order gas phase < *n*-heptane < THF. Thus, the use of a moderately polar solvent is recommended.

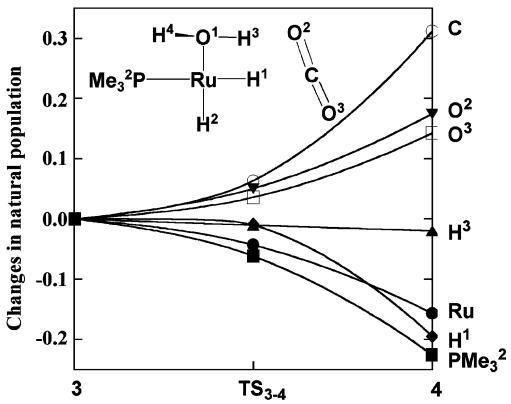

Figure 6. Population changes by the nucleophilic attack of the hydride ligand to carbon dioxide in *cis*-$Ru(H)_2(PMe_3)_3(H_2O)(CO_2)$. A positive value represents an increase in population and vice versa.

The Reason Water Molecules Accelerate the Hydride Attack to Carbon Dioxide. It is of considerable interest to clarify the reason for the very low activation barrier of the hydride attack. As shown in Figure 6, not only the C atomic population but also the O atomic population considerably increase and the H^1 atomic population considerably decreases in this step. The Ru atomic population considerably decreases, also. This is because the donating hydride ligand is removed

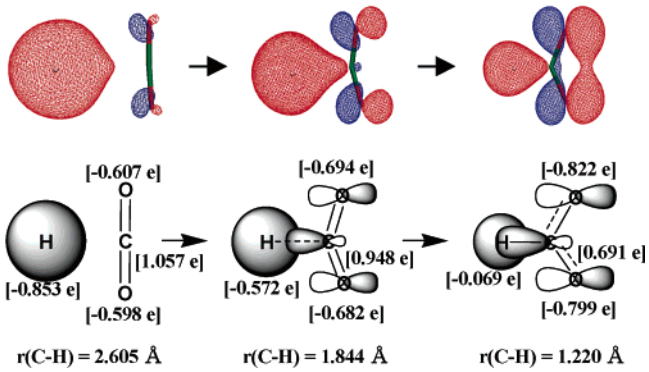

Figure 7. Population changes by the nucleophilic attack of hydride (H^-) to free carbon dioxide. NBO populations are given. The geometry of this model system was taken to be the same as that of the nucleophilic attack in *cis*-$Ru(H_2)(PMe_3)_3(H_2O)(CO_2)$.

Scheme 6

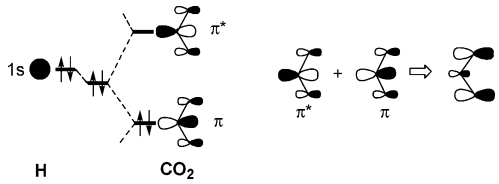

from the Ru center to carbon dioxide, which weakens the charge transfer from the hydride ligand to the Ru center. These population changes are consistent with our understanding that the nucleophilic attack of the hydride ligand to carbon dioxide takes place in this step. To understand well these population changes, we investigated the nucleophilic attack of bare hydride to carbon dioxide, as shown in Figure 7, where the geometry of the H- - -CO_2 moiety was taken to be the same as that of the full reaction system, $Ru(H)_2(PMe_3)_3(H_2O)(CO_2)$. Interestingly, not only the C atom but also the O atom become more negatively charged in the model reaction, as was observed in Figure 6. This is because the hydride 1s orbital overlaps with the π^* orbital of carbon dioxide in a bonding way, into which the π orbital of carbon dioxide mixes in an antibonding way because the π orbital is at lower energy than the hydride 1s orbital, as schematically shown in Scheme 6.[29] Actually, a similar molecular orbital is observed in the real reaction system; as shown in Figure 8A, the H 1s orbital, which is localized on the H ligand in **3**, starts to overlap with the π^* orbital of carbon dioxide in $\mathbf{TS_{3-4}}$ and then the p orbital of the O atom becomes considerably large in **4**. This orbital mixing considerably increases the negative charge on the O atoms. As a result, the hydrogen bond between the O atom of CO_2 and the H atom of the water molecule becomes stronger, as the reaction proceeds. Actually, the H- - -O distance between the aqua ligand and CO_2 becomes shorter, as the nucleophilic attack proceeds. Also, the bonding overlap between the H atom of a water molecule and the O atom of CO_2 becomes large, as shown in Figure 8B, as the reaction proceeds. This hydrogen bond contributes to the stabilization of the transition state and the product. It is of considerable interest to show how much the hydrogen bond contributes to the stabilization energy. The strength of the hydrogen bond is evaluated as follows: In **3** and **4**, the orientation of H_2O is rotated by 90° so as to place the H atom at a position distant from CO_2, in which the hydrogen bond is not formed, as shown in Scheme 7A. This orientation change induces the steric repulsion between PMe_3 and H_2O. The increase in the steric repulsion is estimated by calculating the assumed geometry of $Ru(H)_2(PMe_3)_3(H_2O)$, in which the orientation of H_2O is rotated by 90°, as shown in Scheme 7B. The energy difference between the system with the hydrogen bond and that without the hydrogen bond increases from 6.0 kcal/mol in **3** to 11.6 kcal/mol in $\mathbf{TS_{3-4}}$ and 22.8 kcal/mol in **4**. The steric repulsion is estimated to be 3.3 kcal/mol in **3**, 3.7 kcal/mol in $\mathbf{TS_{3-4}}$, and 5.3 kcal/mol in **4**. Thus, the stabilization energy by the hydrogen bond is 2.7 kcal/mol in **3**, but increases to 5.9 kcal/mol in $\mathbf{TS_{3-4}}$ and 17.5 kcal/mol in **4**. From these results, it is clearly concluded that the transition state and the product are considerably stabilized by the hydrogen bond between CO_2 and the aqua ligand.

Also, another interesting feature is observed in the C−H bonding region between the H ligand and CO_2, as shown in Figure 8A. In the product **4**, the H 1s orbital interacts with the empty d_σ orbital of the Ru center to form an agostic interaction. This typical agostic interaction between the C−H bond of formate and the empty d orbital of the Ru center also contributes to the stabilization of **4**.

In conclusion, the H attack to carbon dioxide easily takes place in the presence of water molecules by the hydrogen bond and the agostic interaction of the C−H bond with the Ru center.

Nucleophilic Attack of Hydride in the Presence of Alcohol and Amine. From the above discussion, we can expect that the hydride attack to carbon dioxide is accelerated by the molecule that has a lone pair orbital utilized for coordination with the Ru center and a proton-like hydrogen atom utilized for a hydrogen bond with the O atom of CO_2. Methanol and dimethylamine are good candidates for such a molecule. Here, we investigated the hydride attack in the presence of methanol, ammonia, and dimethylamine. As shown in Figure 9, the H−N distance between dimethylamine and CO_2 becomes shorter as the H attack proceeds. This geometry change is essentially the same as that of the reaction in the presence of water molecules. Almost the same geometry changes are observed in the NH_3 and methanol complexes (see Supporting Information Figures S2 and S3). The activation barrier was evaluated to be 2.1, 2.1, 2.9, and 3.1 kcal/mol for water, methanol, ammonia, and dimethylamine complexes, respectively, with the DFT method. These activation barriers are similar to or slightly larger than that of the reaction of the aqua complex. Although the reaction of the methanol complex is as exothermic as that of the aqua complex, that of the dimethylamine complex is more exothermic but that of the ammonia complex is less exothermic than that of the aqua complex; the reaction energy is −2.9, −2.6, +0.6, and −3.7 kcal/mol for aqua, methanol, ammonia, and dimethylamine complexes, respectively, where the DFT-calculated values are given. Thus, it is clearly concluded that not only a water molecule but also a Lewis base possessing a proton-like H atom are useful to accelerate the hydride attack to CO_2.

Possibilities That the Other Elementary Processes Participate in the Catalytic Cycle. We also examined whether the other elementary process participates in the catalytic cycle. One of such candidates is the possibility that the CO_2 insertion into the Ru−H bond is accelerated by the presence of water molecules. One water molecule interacts with the O atom of CO_2, which coordinates with the Ru center, as shown in Figure 10, because this O atom is less congested than the other O atom of CO_2. A similar interaction of water with CO_2 was previously proposed.[13] The O−H distance between H_2O and CO_2 is 1.87 Å in the reactant and becomes somewhat shorter as the CO_2 insertion proceeds. This geometry change suggests that the hydrogen-bonding interaction between H_2O and CO_2 becomes stronger in the CO_2 insertion to stabilize the transition state and

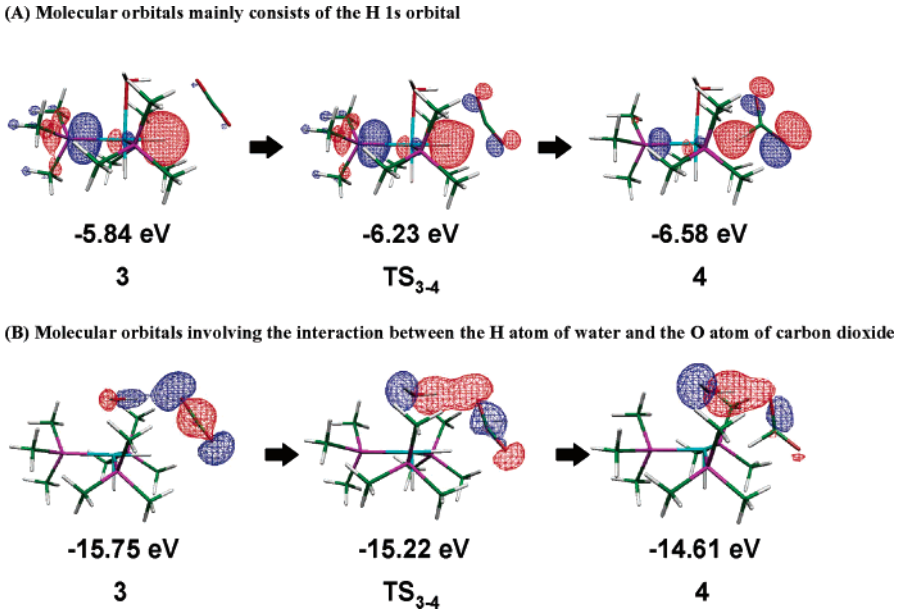

Figure 8. Changes of the Kohn−Sham orbital by the nucleophilic attack of the hydride ligand to carbon dioxide in *cis*-$Ru(H)_2(PMe_3)_3(H_2O)(CO_2)$.

Scheme 7

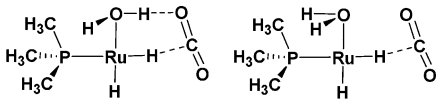

(A) H_2O rotation in $Ru(H)_2(PMe_3)_3(H_2O)(CO_2)$

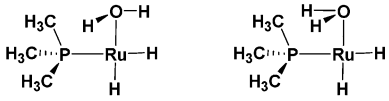

(B) H_2O rotation in $Ru(H)_2(PMe_3)_3(H_2O)$

the product. The activation barrier is evaluated to be 5.4 and 14.7 kcal/mol with the DFT and MP4(SDQ) methods, respectively. These values are moderately smaller than the CO_2 insertion in the absence of water molecules but considerably larger than the hydride attack to carbon dioxide. Moreover, the reaction is considerably endothermic, like that in the absence of water molecules; in other words, the deinsertion of carbon dioxide more easily takes place than the insertion. This means that the dihydrogen coordination necessarily occurs to complete the hydrogenation reaction. Thus, it is concluded that the CO_2 insertion is less favorable than the H attack in the presence of water molecules.

The other possible role of the water molecule is to participate in the formation of formic acid by adding a proton to formate and taking a proton from the dihydrogen molecule, as shown in Scheme 8.[8,31] We investigated this water-assisted proton relay reaction, as shown in Figure 11. However, the activation barrier was evaluated to be 13.3 kcal/mol with the DFT method, which is much larger than that (7.3 kcal/mol) of the simple metathesis by 6.0 kcal/mol. From these results, it is concluded that the usual metathesis more favorably occurs than this water-assisted proton relay and that this process is not responsible for acceleration by water molecules.

We must consider the other possible isomer of the dihydrogen complex in which the dihydrogen molecule takes a position trans to hydride, as shown in Scheme 9. This complex is expected to be easily formed through substitution of a water molecule for a dihydrogen molecule in **4**. However, the metathesis does not take place starting from this dihydrogen complex, as was reported previously.[12b] The reason was easily interpreted in terms of the trans influence of the hydride ligand; the product of such a metathesis is not stable because two hydride ligands take positions trans to each other.

Conclusions

Ru-catalyzed hydrogenation of carbon dioxide to formic acid was theoretically investigated with DFT and MP2 to MP4(SDQ) methods, to clarify the reaction mechanism in the absence of water molecules and the reasons that a small quantity of water significantly accelerated this hydrogenation reaction. Several interesting differences are observed between the reactions in the presence and the absence of water molecules, as follows: The active species is *cis*-$Ru(H)_2(PMe_3)_3$ in the absence of water molecules but *cis*-$Ru(H)_2(PMe_3)_3(H_2O)_2$ in the presence of water molecules. The CO_2 adduct is also different; in the presence of water molecules, CO_2 cannot directly interact with the Ru center but interacts with the hydride and aqua ligands, while carbon dioxide directly coordinates with the Ru center to afford $Ru(H)_2(\eta^2\text{-}CO_2)(PMe_3)_3$ in the absence of water molecules. As a result, the Ru-(η^1-formate) intermediate is produced through CO_2 insertion in the absence of water molecules but through nucleophilic attack of the H ligand to CO_2 in the presence of water molecules. The nucleophilic attack easily takes place with a small activation barrier and much less endothermicity (or small exothermicity in supercritical carbon dioxide). The rearrangement of the formate moiety to afford $RuH(\eta^1\text{-}OCOH)(PMe_3)_3(H_2O)$ also easily takes place with a small activation barrier and an extremely large exothermicity. This process stabilizes the reaction system very much; in other words, the back reaction is suppressed by this unimolecular process. After this rearrangement, the dihydrogen molecule coordinates with the Ru center, which needs a moderate activation barrier. The final step is metathesis, which occurs in essentially the same manner as that of the reaction in the absence of water molecules. In the potential energy surface, the metathesis is the rate-determining step. Its

(31) Casey, C. P.; Johnson, J. B.; Singer, S. W.; Cui, Q. *J. Am. Chem. Soc.* **2005**, *127*, 3100.

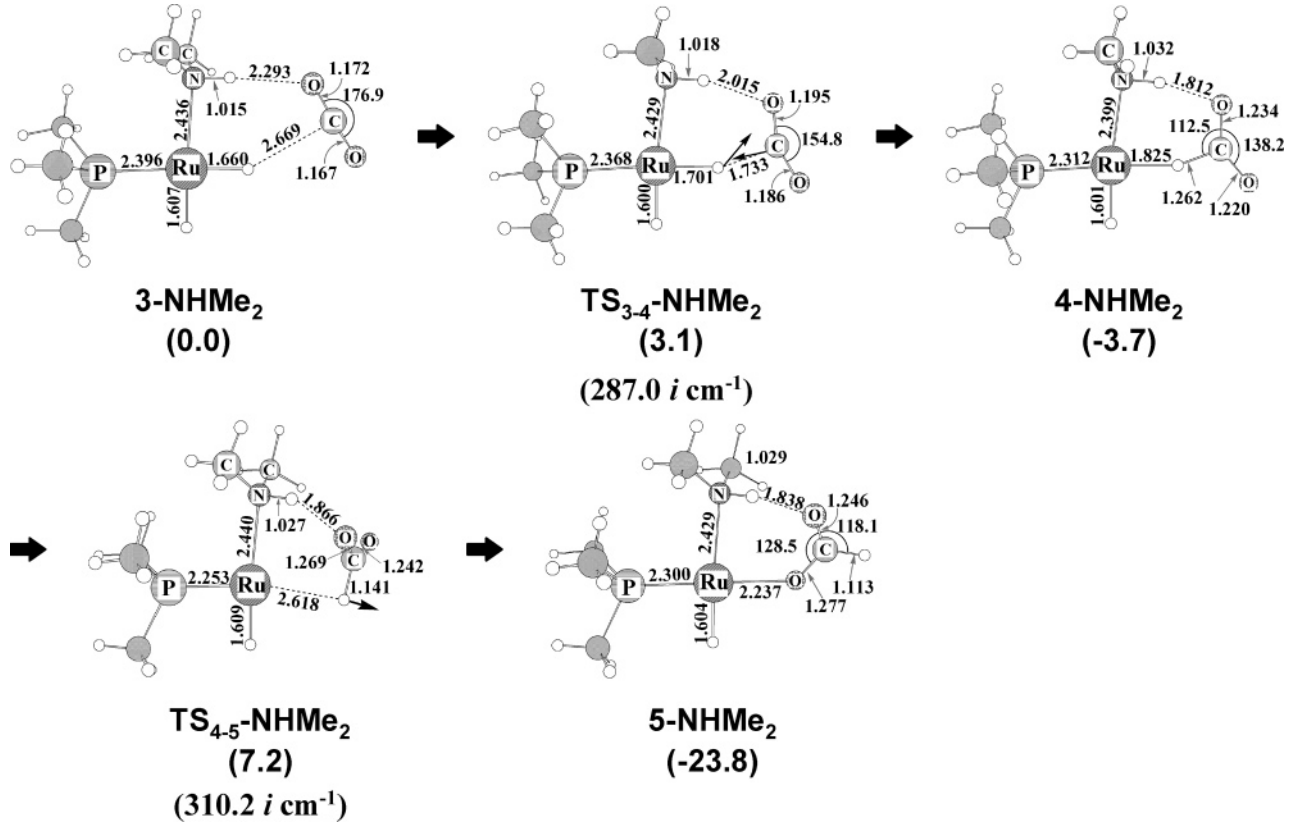

Figure 9. Geometry changes by the nucleophilic attack of the hydride ligand to the C center of carbon dioxide in *cis*-$Ru(H)_2(PMe_3)_3(NHMe_2)(CO_2)$. In parentheses are the imaginary frequencies. Arrows in **TS_{3-4}-NHMe$_2$** represent important movements of nuclei in the transition state.

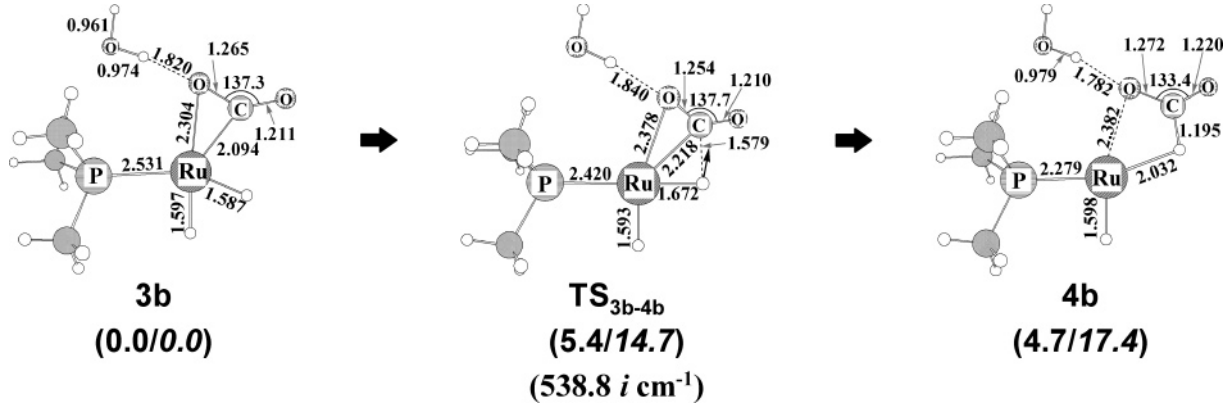

Figure 10. Geometry changes by the insertion of carbon dioxide into the Ru−H bond of *cis*-$Ru(H)_2PMe_3)_3(CO_2)$ in the presence of water molecule. In parentheses are the imaginary frequencies. Arrows in **TS_{3b-4b}** represent important movements of nuclei in the transition state. In parentheses are energy changes; numbers in normal font represent the DFT-calculated energy change and those in italic font represent the MP4(SDQ)-calculated energy change (kcal/mol unit).

Scheme 8

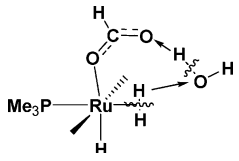

activation barrier is much smaller than that of the CO_2 insertion into the Ru−H bond, which is the rate-determining step in the absence of water molecules. In the free energy surface, on the other hand, the coordination of a dihydrogen molecule with the Ru center is rate-determining. Although its activation free energy change in the gas phase is estimated to be similar to that of the CO_2 insertion, the real value of the free energy change should be smaller than that of CO_2 insertion because the entropy decreases much less here than in the gas phase.[32] Thus, it should be clearly concluded that the presence of water molecules accelerates the hydrogenation in either potential energy changes or free energy changes.

The acceleration by water molecules arises from the fact that the Ru-(η^1-formate) intermediate is easily formed through nucleophilic attack of the H ligand to CO_2 in the presence of water molecules. This is because the hydrogen-bonding interac-

(32) The entropy considerably decreases when an adduct is formed in the gas phase because the partition functions of the translation and rotation movements considerably decrease. On the other hand, those movements are highly suppressed in solution. This means that the entropy decrease in the gas phase is much larger than that in solution, in general.

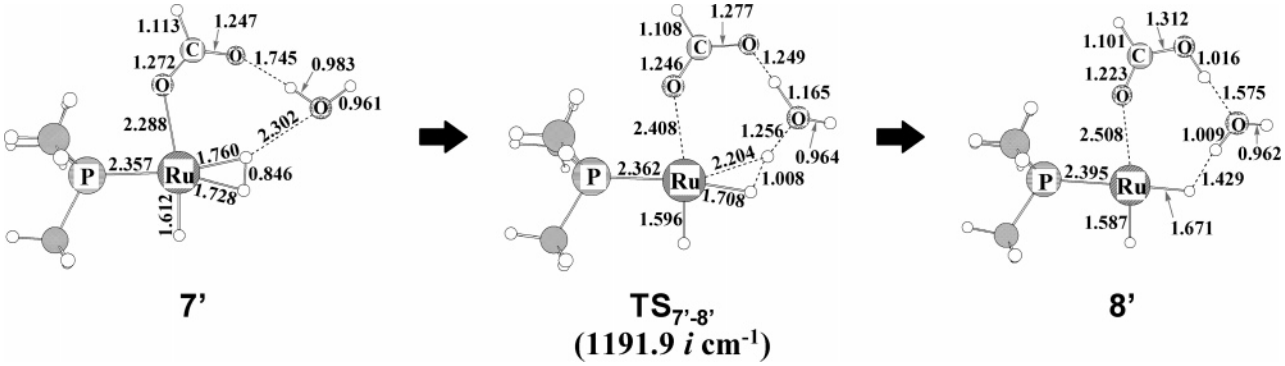

Figure 11. Geometry changes by the water-assisted proton relay reaction of Ru(H)(η^1-OCOH)(PMe_3)$_3$ with a dihydrogen molecule. Bond lengths are in angstroms and bond angles in degrees. In parentheses is the imaginary frequency of the transition state.

Scheme 9

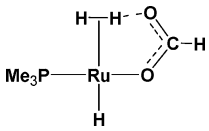

tion between the H atom of water and the O atom of carbon dioxide becomes stronger in the nucleophilic attack to decrease the activation barrier and the endothermicity. The other reason for the acceleration is that the back reaction from Ru(H)(HCO_2)-(PMe_3)$_3$(H_2O) to the Ru(H)$_2$(PMe_3)$_3$(H_2O)(CO_2) is suppressed by the isomerization of the formate moiety in the presence of the water molecule. In the absence of water molecules, the coordination of the dihydrogen molecule with the Ru center must occur to suppress the deinsertion of CO_2. This coordination process is much exothermic, but this process occurs less easily than the isomerization of the formate moiety because the concentration of dihydrogen molecules is not sufficiently large in the reaction solution and also this is a bimolecular process, which occurs less easily than the unimolecular process, such as the isomerization of the Ru-(formate) moiety. Not only water molecules but also alcohols and amines can accelerate the nucleophilic attack in the same manner.

Acknowledgment. This work was financially supported by Grants-in-Aid on basic research (No. 15350012), Priority Areas for "Reaction Control of Dynamic Complexes" (No. 420), Creative Scientific Research, and NAREGI project from the Ministry of Education, Science, Sports, and Culture, Japan. Some of theoretical calculations were performed with SGI workstations at the Institute for Molecular Science (Okazaki, Japan), and some of them were carried out with PC cluster computers in our laboratory.

Supporting Information Available: Cartesian coordinates of important species including transition states. Energy changes of the CO_2 insertion into the Ru−H bond calculated with various computational methods and geometry changes by the nucleophilic attack of the H ligand to CO_2 in Ru(H)$_2$(PMe_3)$_3$(MeOH)(CO_2) and Ru(H)$_2$(PMe_3)$_3$(NH_3)(CO_2). This material is available free of charge via the Internet at http://pubs.acs.org.

OM060307S